



Cite this: *Integr. Biol.*, 2014,  
6, 1122

## Three-dimensional intestinal villi epithelium enhances protection of human intestinal cells from bacterial infection by inducing mucin expression<sup>†</sup>

Si Hyun Kim,<sup>a</sup> Meiyiing Chi,<sup>b</sup> Banya Yi,<sup>a</sup> So Hyun Kim,<sup>b</sup> Seunghan Oh,<sup>b</sup> Younghoon Kim,<sup>c</sup> Sungsu Park<sup>\*d</sup> and Jong Hwan Sung<sup>\*a</sup>

Current *in vitro* cell culture models do not reflect human physiology, and various efforts have been made to enhance existing models. Reconstitution of three-dimensional (3D) tissue structure has been one of the strategies, since 3D tissue structure provides essential cellular environmental cues for cell functions. Previously, we developed a novel hydrogel microfabrication technique for constructing an accurate 3D replica of human intestinal villi epithelium. In this study, genetic and physiological properties of the 3D villi model were examined to gain a better insight into the barrier function of gut epithelium and its interaction with microbes. Gene expression study of Caco-2 on the 3D villi scaffold revealed that expression of MUC17, which is one of the transmembrane mucins, was highly enhanced in the 3D villi model, compared to a monolayer culture. Cells on the scaffold were almost immune to bacterial infection, while MUC17 knockdown in Caco-2 cells restored bacterial infectivity. The 3D villi model also exhibited changes in the barrier function compared to the 2D model, manifested by changes in transepithelial electrical resistance (TEER) and permeability of FITC-dextran. Knockdown of MUC17 resulted in reduction of tight junction protein expression and further increase in permeability, suggesting an important role of MUC17 in the barrier function against pathogens and xenobiotics. Our study suggests that mimicking the 3D tissue architecture of the small intestine induces physiological changes in human intestinal cells.

Received 7th July 2014,  
Accepted 20th August 2014

DOI: 10.1039/c4ib00157e

[www.rsc.org/ibiology](http://www.rsc.org/ibiology)

### Insight, innovation, integration

In an effort to enhance existing *in vitro* models and predict human responses better, microfabrication technology has been increasingly applied to reproduce the *in vivo* tissue micro-environment. Previously we reported a novel hydrogel microfabrication method to mimic the 3D structure of human intestinal villi. Here, by studying gene expression and bacterial adhesion as well as drug permeability in the 3D villi model, we show that mimicking the 3D geometry induces physiological changes in human intestine cells related to barrier function against bacteria and xenobiotics. Integration of the microfabrication technique with a cell model can provide important insights into the effect of tissue microenvironment on cell physiology, as well as the mechanism related to the interaction of human intestine with gut microbiota.

## 1. Introduction

Existing *in vitro* models of the gut epithelium often fail to reproduce human physiology, for example drug absorption,<sup>1</sup>

drug–drug interaction,<sup>2</sup> and viral infectivity.<sup>3</sup> Therefore, a great amount of effort has been made to enhance current models to recapitulate the complex physiology of human organs.<sup>4</sup> Caco-2 cells, a human colon epithelial cancer cell line, exhibit some of the characteristics of the human small intestine, such as tight junctions between cells, drug transporter and efflux proteins, and phase II conjugation enzymes, and have been widely used as an *in vitro* model for drug absorption as well as bacterial infection.<sup>5,6</sup> However, several serious limitations of the Caco-2 monolayer cell model exist, such as low expression of P450 enzyme,<sup>5</sup> and almost complete lack of mucus production.<sup>7</sup> Also the permeability of slowly absorbed drugs in Caco-2 model correlates poorly with the absorption rates in humans, and it was suggested that this lack of physiological relevance might be

<sup>a</sup> Department of Chemical Engineering, Hongik University, Seoul, Korea.  
E-mail: jhsung22@hongik.ac.kr

<sup>b</sup> Department of Chemistry and Nano Sciences (BK21 plus), Global Top 5 Program, Ewha Womans University, Seoul, Korea

<sup>c</sup> BK21 Plus Graduate Program, Department of Animal Science and Institute Agricultural Science & Technology, Chonbuk National University, Jeonju, 561-756, Korea

<sup>d</sup> School of Mechanical Engineering, Sungkyunkwan University, Suwon, Korea.  
E-mail: nanosingapore@gmail.com

† Electronic supplementary information (ESI) available. See DOI: 10.1039/c4ib00157e

due to the lack of three-dimensional tissue architecture of human small intestine.<sup>1</sup>

In mammalian tissues, cells are surrounded by a complex physiological milieu that provides cells with various signals for appropriate growth, differentiation, and function. These signals include soluble factors, cell-cell or cell-matrix interaction, and mechanical forces in the three-dimensional (3D) environment.<sup>8–10</sup> Among these factors, 3D tissue structure is thought to play an important role in determining the physiological function of cells.<sup>11,12</sup> Recent development in microtechnology has allowed fabrication of microscale structures of *in vivo* tissues, thus providing cells with a more physiologically realistic environment than conventional 2D cell culture models.<sup>13,14</sup> Cells have often shown enhanced function that is closer to their *in vivo* status, when they were provided with an appropriate 3D environment of the liver,<sup>15,16</sup> breast cancer,<sup>17,18</sup> heart,<sup>19</sup> and bone.<sup>20</sup>

The small intestine also comprises complex physiological features, including chemical signaling between multiple cell types, mechanical movement, symbiotic microbes, and unique 3D structure manifested by the crypts and villi on the intestinal wall.<sup>21–23</sup> Because current 2D models of the intestine lack many of the physiological features and do not accurately reproduce intestinal functions, there have been active research efforts to create 3D models of the small intestine.<sup>24–30</sup> In these studies, human intestinal cells were cultured on a 3D collagen matrix with mucus producing and stromal cells,<sup>24</sup> with immunocompetent macrophages and dendritic cells,<sup>25</sup> in the presence of fluidic shear and mechanical strain.<sup>29,30</sup> Although these studies have shown that intestinal epithelial cells cultured in 3D resemble *in vivo* intestinal epithelium better than the conventional 2D model, these models do not fully recapitulate the actual geometry of intestinal tissue. The intestinal epithelium contains a unique topography of villi and crypts, which are finger-like projections with a height of 500–1000 µm and well-like invaginations that are known to increase the absorptive surface area and affect the physiology of the epithelial cells.<sup>1,31</sup> However, this unique 3D geometry of intestinal epithelium is not reflected in the above-mentioned models. Microfabrication techniques have been used to simulate this unique topography and study its effect on the cell physiology by creating an analog of intestinal crypts<sup>32,33</sup> and villi.<sup>34</sup> While these biomimetic 3D intestine models have successfully simulated the unique topography of intestinal epithelium, yet in-depth studies on the physiology of the 3D models are lacking. Recent studies have demonstrated the advantages of the intestinal villi structure made of a synthetic and biodegradable hydrogel,<sup>35</sup> using co-culture of intestinal epithelial cells and several bacterial populations.<sup>36</sup> However, the use of a synthetic hydrogel instead of a natural extracellular matrix (ECM) hydrogel may limit the physiological relevance of such models.

Previously, we developed a novel method to fabricate a 3D collagen scaffold having the exact geometry of the human intestinal villi.<sup>37</sup> This method enables replication of the exact geometry and the density of the human intestinal villi with a soft extracellular matrix hydrogel such as collagen. When the human intestinal Caco-2 cells were cultured on this villous hydrogel scaffold, cells grew and migrated to form a 3D structure with a strong resemblance to the

human intestinal villi. In a subsequent drug absorption study, it was verified that the permeability coefficients measured in this 3D model was closer to the *in vivo* values than the permeability measured using a conventional 2D model.<sup>38</sup> It has been speculated that the 3D villi scaffold facilitated cellular differentiation and absorption characteristics similar to those of mammalian tissues, but further physiological studies explaining these phenotypic changes are lacking.

Herein, gene expression changes of Caco-2 cells on the 3D scaffold were investigated using transcriptome analysis. High expression of MUC17 on the scaffold, one of the transmembrane mucins, was confirmed by immunostaining and RT-PCR. The effect of the changes in MUC17 expression on bacterial infection was studied by challenging Caco-2 cells on the scaffold with/without siMUC17 treatment with *Salmonella typhimurium* and *Escherichia coli* O157:H7. The effect of MUC17 expression on the barrier function of Caco-2 cells was also studied by measuring transepithelial electrical resistance (TEER) and the permeability of FITC-dextran through the intestinal epithelium. The results of this study indicate that mimicking the 3D tissue structure of the small intestine with natural ECM induces physiological changes in Caco-2 cells related to the barrier function against pathogens and xenobiotics.

## 2. Results

### 2.1. Cell growth and MUC17 expression in the 3D villi model

The 3D villi scaffold was fabricated from collagen using a sacrificial alginate mold, and Caco-2 cells were seeded on the collagen scaffold and grown until they covered the scaffold, after which various experiments were performed (Fig. 1(a)). Fig. 1(b) shows the SEM images of the fabricated scaffold in PDMS with a height of about 500 µm. When Caco-2 cells were seeded onto the villi scaffold, the curved geometry of the scaffold caused most of the cells to settle in the lower crypt areas. After three days of seeding, the cells completely covered the crypt

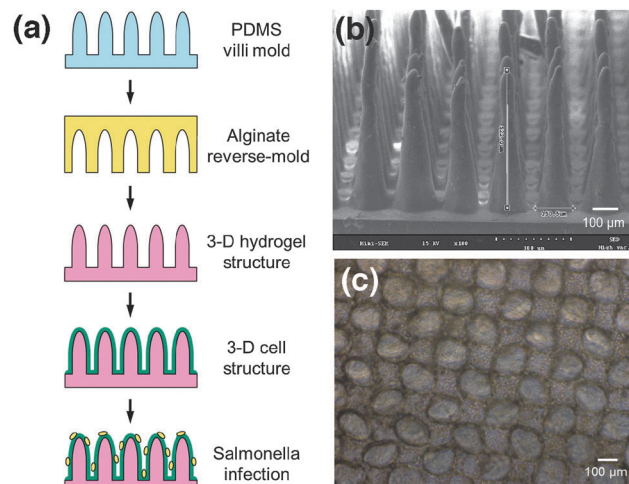
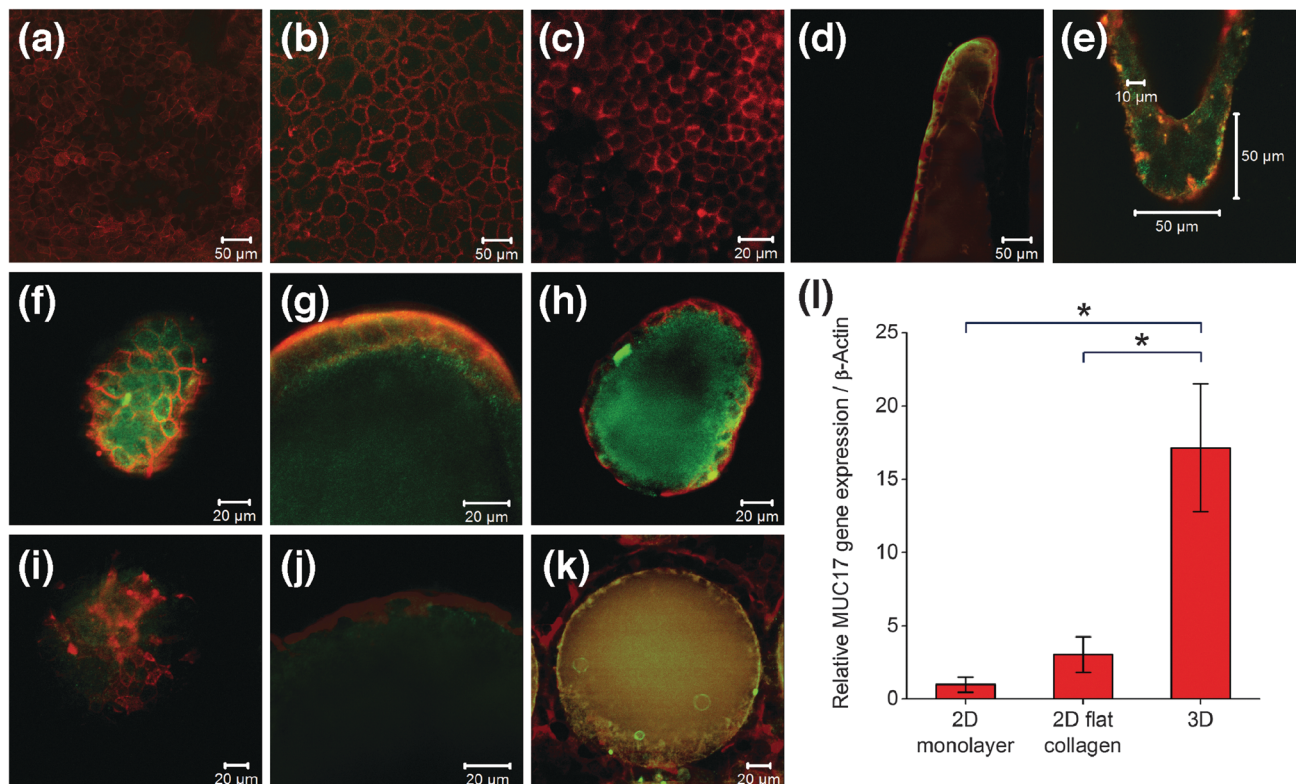


Fig. 1 Fabrication of a 3D villi model; (a) process diagram for fabricating a 3D villi scaffold and culturing Caco-2 cells; (b) SEM image of fabricated villi in PDMS; (c) bright field image of Caco-2 cells grown on the 3D villi scaffold.



**Fig. 2** Expression of MUC17 in Caco-2 cells. Expression of MUC17 in Caco-2 cells (red: actin, green: MUC17) in (a) 2D culture (day 3); (b) 2D culture (day 20); (c) 2D culture on a collagen substrate, (d) 3D culture (a villus tip, side view), and (e) 3D culture (a crypt, side view). Top view figures showing the expression of MUC17 in 3D Caco-2 cells on (f) top; (g) side; (h) middle of the 3D villi scaffold, and in MUC17 knockdown Caco-2 cells on (i) top; (j) side; (k) middle of the 3D villi scaffold; (l) RT-PCR comparison of the MUC17 mRNA expression level in Caco-2 cells cultured in 2D monolayer, 2D monolayer on collagen gel, 3D villi scaffold.

areas and started migrating up to the villi. After two weeks, approximately 50% of the villi were completely covered with cells, and after about 20 days all of the villi were completely covered. Fig. 1(c) shows the bright field images of Caco-2 cells on the 3D scaffold and in the 2D monolayer, respectively. Confocal images of the 3D villi with or without the cells have been provided in the previous paper.<sup>37</sup> Cells on the villi were viable for at least 30 days from the initial seeding, after which some cells were observed to detach from the scaffold. When Caco-2 cells on the 3D villi scaffold were treated with siMUC17, in order to examine the effect of MUC17 expression on growth and morphology of Caco-2 cells, neither the growth rate nor cell morphology were affected.

Whole transcriptome analysis of the cells showed that the gene expression of cells in the 3D villi model changed significantly from that of the 2D culture. In particular, the expression of the mucin gene family changed several fold (see ESI† for further details). To study the effect of collagen and 3D villi structure on the expression of MUC17 in the 3D villi model, immunostaining of MUC17 was performed on Caco-2 cells cultured under three different conditions. A monolayer culture on a membrane support, a monolayer culture on a collagen substrate, or a 3D cell culture on the villi model. The expression of MUC17 in cells cultured as a monolayer on a membrane for three days (Fig. 2(a)) or twenty days (Fig. 2(b)) was negligible.

Cells cultured as a monolayer on a collagen substrate also showed a negligible amount of MUC17 expression (Fig. 2(c)). This result shows that MUC17 expression is affected more by the 3D tissue architecture than the presence or absence of a collagen substrate itself. On the other hand, a significant amount of MUC17 expression was detected in cells cultured on the 3D villi scaffold for twenty days, both in the villi (Fig. 2(d)) and the crypts area (Fig. 2(e)). Top view figures also show high expression of MUC17 in the 3D villi model (Fig. 2(f)–(h)). It was notable that green fluorescence was also observed inside the collagen gel as well as the cell surface. Although MUC17 is membrane bound mucin, a secreted form of MUC17 also exists.<sup>39</sup> The green fluorescent signal inside the collagen gel probably originated from MUC17 which was secreted from Caco-2 cells and diffused in the collagen gel. Knockdown of MUC17 by siRNA is displayed in Fig. 2(i)–(k). When cells on the 3D villi scaffold were treated with siMUC17 during the entire period of the 20 day culture, MUC17 expression was significantly reduced. It is also notable that the cells treated with siRNA displayed weakened tight junctions between the cells, and this caused rhodamine phalloidin, the red stain for actin, to diffuse across the cell layer into the villi structure (Fig. 2(k)). The relative mRNA expression level was also compared by RT-PCR (reverse transcription polymerase chain reaction). Fig. 2(l) shows that expression of MUC17 in Caco-2 cells on the 3D villi scaffold was

substantially higher than the same cells in the 2D monolayer, either cultured on a membrane support or a collagen substrate. Culturing Caco-2 cells in a monolayer on a collagen substrate also increased MUC17 expression slightly, but the extent of expression was significantly lower than the case of the 3D villi model.

## 2.2. Bacterial invasion and infection assays

To study the protective effect of MUC17 expression on Caco-2 against bacterial infection, cells either in a 2D monolayer on a membrane or on the 3D villi scaffold were co-incubated with *S. typhimurium*, and the number of bacterial cells that invaded into Caco-2 cells was counted. Invasion by this microorganism was more easily identified in Caco-2 cells in a monolayer than in Caco-2 cells on the 3D villi scaffold. The pattern of bacterial invasion into the host cells in a 2D monolayer seemed to be not affected by culture periods (3 and 20 days), as shown in Fig. 3(a) and (b). Caco-2 cells cultured in the monolayer of collagen were also invaded by *S. typhimurium* (Fig. 3(c)). This result shows that collagen itself does inhibit bacterial infection. This is further supported by the result shown in Fig. 2(l), which shows only a slight increase in MUC17 expression in Caco-2 cells when they were grown in the collagen monolayer. In contrast, in the case of the 3D villi model, bacterial invasion was limited only to a few host cells on the crypt part of the 3D scaffold, while no invasion was observed in cells on the villi tips (Fig. 3(d) and (e)), suggesting that the Caco-2 cells on the 3D villi scaffold was more immune to bacterial invasion than the same cells in a 2D monolayer. To confirm the role of MUC17 in protection against pathogens, MUC17 was knocked down by treating with siRNA. The siMUC17-treated cells on the 3D villi scaffold were invaded more by the pathogen, and invasion was observed in the host cells in both crypts and villi tips (Fig. 3(f) and (g)). The number of invaded bacterial cells per villus was increased about 10-fold after siMUC17 treatment, as shown in Fig. 3(h). These results suggest that the 3D architecture mimicking the intestinal villi plays a greater role than the presence of the collagen substrate in inducing physiological changes in Caco-2 cells.

SEM images were taken to examine the surface of Caco-2 cells on the villi scaffold with and without siMUC17 treatment. In the case of Caco-2 cells in the 3D villi model, no bacterium was seen on the cell surface, while the uniform formation of microvilli on the cell surface was observed (Fig. 3(i) and (j)). In contrast, siMUC17-treated cells on the 3D villi scaffold displayed a cracked and damaged surface, with less uniform formation of microvilli (Fig. 3(k) and (l)). On the surface of the Caco-2 cells, we were able to locate the bacteria invading the cell surface. Fig. 3(l) shows the invagination of *S. typhimurium* by the host cells, which is often found in the infected host cells. In a separate experiment using another bacterial strain *E. coli* O157:H7, the bacteria also infected the 2D monolayer cells but did not infect the 3D cell model (ESI†). These results, taken together with the MUC17 expression result, suggest that the 3D villi structure enhances expression of MUC17, which inhibits bacterial infection.

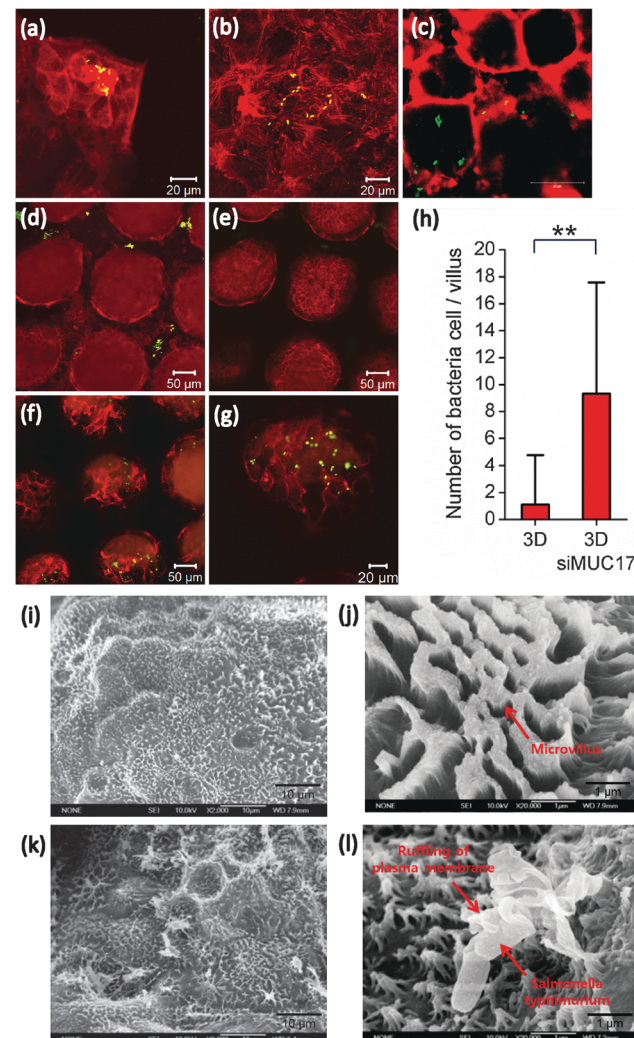


**Fig. 3** *S. typhimurium* infection in 3D with/without siMUC17 treatment. Fluorescence image of Caco-2 cells co-incubated with the microorganism under different culture conditions: (a) 2D culture at day 3; (b) 2D culture at day 20; (c) 2D culture on a collagen substrate at day 20; (d) the crypt part of 3D villi at day 20; (e) the villus tips of 3D villi at day 20; (f) the villus tips of 3D culture treated with siMUC17 at day 20; and (g) a single villus of 3D culture treated with siMUC17 at day 20 (red: actin, green: *S. typhimurium* labeled with GFP); (h) number of invaded bacterial cells per villus (\*\*  $p < 0.001$ ). SEM images of the surface of Caco-2 cells on the 3D villi scaffold at different magnifications; (i)  $\times 2000$ ; (j)  $\times 20\,000$ . (k) SEM image of the surface of siMUC17-treated Caco-2 cells on the 3D villi scaffold and (l) invagination of *S. typhimurium* by the host cells at 2000 magnification.

## 2.3. Barrier function of the 3D villi model

To examine the integrity of tight junctions in the cells on the 3D villi scaffold, we performed immunostaining for occludin, which is an integral plasma membrane protein as well as a main component of tight junctions. In the 3D villi model, occludin was clearly observed between the cells (Fig. 4(a)–(c)), verifying that the tight junction was uniformly intact across the whole surface of the villi structure. However, it was observed that the occludin expression was weaker in the villi top area than the bottom crypt area, implying that the tight junction might have different integrity depending on the location of the

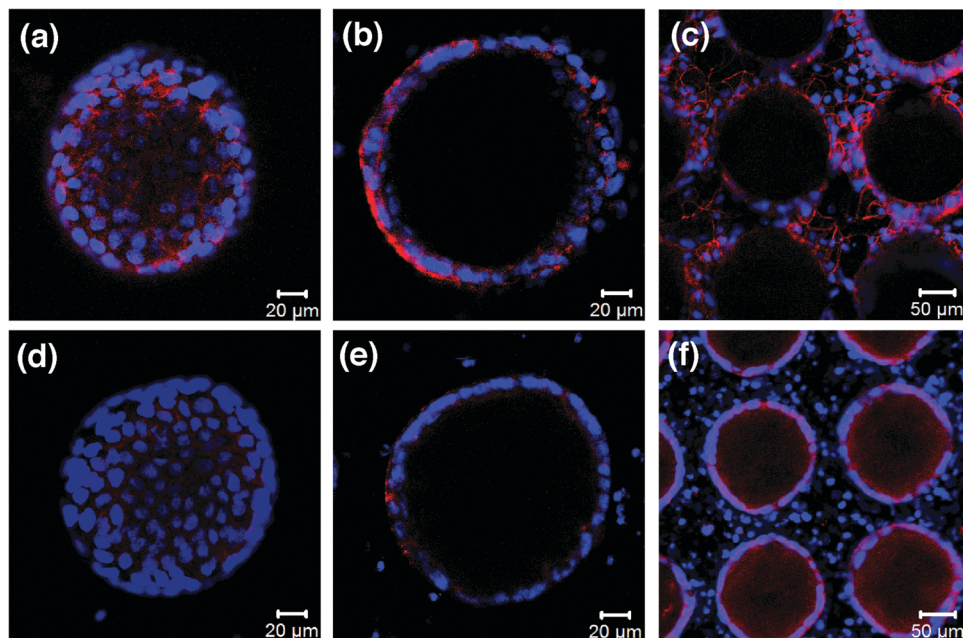


**Fig. 4** Expression of occludin in 3D villi with and without siRNA treatment. Expression of occludin in Caco-2 cells on (a) top; (b) middle; (c) bottom area and expression of occludin in siMUC17-treated Caco-2 cells on (d) top; (e) middle; (f) bottom area of the 3D villi scaffold (red: occludin, blue: DAPI).

3D villi model. Compared to cells in a monolayer ( $ESI^{\dagger}$ ), cells in the crypt area showed a similar level of occludin expression whereas cells on the top and middle parts of the 3D villi scaffold showed lower levels of expression. In contrast, siMUC17 treated Caco-2 cells on the 3D villi scaffold showed significantly reduced levels of occludin expression in all areas (Fig. 4(d)–(f)). In cells on both top and middle parts of the 3D scaffold, occludin expression was significantly weaker, which implies that the tight junction integrity might be compromised when treated with siMUC17.

Epithelial barrier functions of Caco-2 cells in the 2D and 3D villi model were compared by measuring the TEER and permeability of FITC-dextran in a transwell. The result in Fig. 5(b) shows that after 20 days, the TEER in the 3D model was only  $90 \Omega \text{ cm}^2$ , whereas the TEER of the 2D model was about  $260 \Omega \text{ cm}^2$ . At the beginning of the experiment, the TEER of

the 3D villi model was slightly higher than that of the 2D model due to the attachment of the villi scaffold, but over the period of 20 days, the increase of the TEER value was significantly lower in the 3D model compared to the 2D model ( $ESI^{\dagger}$ ). In the study by Yu *et al.*,<sup>38</sup> the 3D model showed a dramatically lower value of TEER than the 2D cell model, and showed much higher permeability to a model drug antipyrine and atenolol compared to the 2D model. In our study, the TEER of the 3D model was also lower than that of the 2D model, and the observed permeability of FITC-dextran was higher in the 3D villi model (about two-fold increase, Fig. 5(c)), with statistical significance ( $p < 0.001$ ). In the case of the 3D villi model treated with siMUC17 for knockdown of the MUC17 gene, the TEER measured after 20 days was only slightly lower than that of a 2D model. Despite the small change in the TEER, the 3D villi model treated

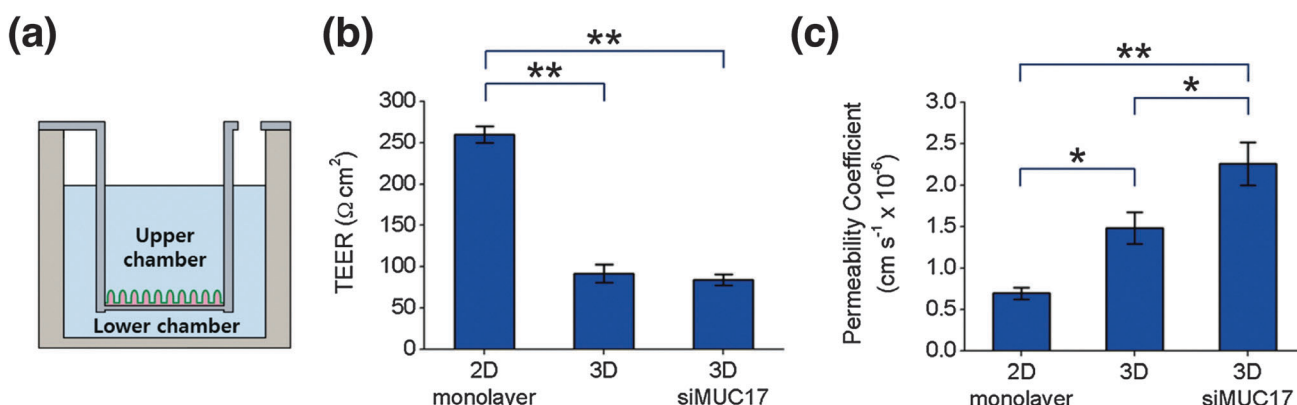


**Fig. 5** TEER and permeability coefficient. (a) A schematic of TEER and permeability measurement in the 3D villi scaffold. (b) TEER values of 2D monolayer and 3D model with/without siMUC17 treatment (\*\*  $p < 0.001$ ). (c) Permeability of FITC-dextran (4 kDa) in 2D monolayer and 3D model with/without siMUC17 treatment (\*  $p < 0.01$ , \*\*  $p < 0.001$ ).

with siRNA showed a higher permeability to FITC-dextran than the untreated 3D model, implying changes in the epithelial barrier integrity.

### 3. Discussion

Previously, we reported that Caco-2 cells were able to proliferate and migrate on the surface of a 3D scaffold mimicking the architecture of human intestinal villi, resulting in a 3D structure resembling the intestinal wall tissue.<sup>37</sup> Several recent studies have indicated that 3D scaffolds made of an extracellular matrix induce changes in the physiology of intestinal cells. In one study, Caco-2 cells were cultured in a 3D in the presence of other cell types, such as HT29 methotrexate cells and stromal cells.<sup>24</sup> Interestingly, this 3D model changed the values of TEER and permeability of several model drugs, apparently caused by the changes in the expression levels of transporter proteins. Another study reports co-culture of Caco-2 cells with macrophages and dendritic cells, and stimulating with proinflammatory factors resulted in a decrease in the TEER value, suggesting changes in the epithelial barrier property.<sup>25</sup> In a study by Kim *et al.*, culturing Caco-2 cells under hydrodynamic shear and periodic mechanical strain mimicking the peristaltic motion of the human gut resulted in the formation of a villi-like structure,<sup>30</sup> with differentiation of Caco-2 in terms of enhanced expression of several differentiation markers including cytochrome P450, villin, sucrose isomaltase and mucins.<sup>29</sup> All these models employed cells arranged in a 3D configuration, but did not resemble the accurate architecture of human gut tissues. In our study, the effect of mimicking the exact geometry of human intestinal epithelium on the physiology of human intestine cells was studied.

The intestinal mucosal surfaces are protected from pathogens and toxic chemicals by various mechanisms. Among these mechanisms, mucins, high molecular weight glycoproteins produced by epithelial cells, provide protection by preventing noxious interactions of epithelial cells with pathogens by providing a physiochemical barrier.<sup>40</sup> Mucins hamper the ability of pathogens to adhere to or invade the surface of epithelial cells, and subsequently block the spread and colonization of bacteria and viruses.<sup>41</sup> Mucin gene families are generally classified into two groups, secreted and membrane-bound mucins, with the main difference being the presence or the absence of a transmembrane domain.<sup>42</sup> Our transcriptome-analysis data suggested that among several mucin genes, MUC17 was highly expressed when Caco-2 cells were cultured on the 3D villi scaffold. A control experiment with 2D Caco-2 cells on a flat collagen gel indicated that the presence of collagen gel also enhances MUC17 expression to some extent, but the effect of the 3D structure was significantly greater. MUC17 has been detected throughout the entire intestinal tract with the highest expression in the duodenum.<sup>42</sup> Our study suggests that the combination of correct tissue architecture with appropriate extracellular matrix signaling induces changes in the expression of mucins by Caco-2 cells.

The bacterial infection study using *S. typhimurium* indicated that the MUC17, which was highly expressed in the 3D villi model, provided protection for the epithelial cells against bacterial infection. This result was further confirmed by the knock-down experiment of the *muc17* gene using siRNA, which restored the bacterial infectivity normally seen in the 2D model. This observation is consistent with recent findings about the protective role of MUC17. In a study using the LS174T cell line, known to have a high level of baseline expression of MUC17, reduced expression of MUC17 was associated with reduced cell aggregation, adherence, and migration.<sup>43</sup> In another study, reduction of MUC17 expression was associated with increased permeability, inducible nitric oxide synthase and cyclooxygenase-2 induction, and enhanced bacterial invasion in response to *E. coli* O157:H7 exposure.<sup>44</sup> We observed a similar trend with exposure of Caco-2 cells to *S. typhimurium* as well as *E. coli* O157:H7, where these microorganisms easily invaded the 2D cell surfaces, but not cells in the 3D villi model (see ESI†). Mucin production is not only related to the protective function against pathogens, but also seems to be associated with progression of diseases such as cancer and inflammatory diseases.<sup>41,45</sup> This evidence suggests that our villi model may serve as a better *in vitro* model for such diseases. A recent study showed that when Caco-2 and HT29-MTX, a mucus producing cell line, were co-cultured in a similar villi scaffold made of a synthetic hydrogel, they enhanced the production of mucus.<sup>35</sup> Another study by the same research group reported that the villi-like topography induced cell differentiation and different microbial species adhered selectively to different locations, depending on the differentiation states of the cells.<sup>36</sup> Our results along with these studies suggest that reproducing the 3D architecture of the intestinal tissue helps recapitulating the phenotypes that are more representative of the native tissue.

The topography of the intestine tissue may have an effect on the absorptive property, as the surface area of the intestinal mucosa is thought to play a role in determining the permeability of drugs, especially for hydrophilic drugs with low permeability.<sup>1</sup> Interestingly, it was observed that cells cultured in the 3D villi model showed a decrease in the TEER compared to the 2D model (Fig. 5(b)). This observation is consistent with previous studies by other groups, where Caco-2 cells grown in a 3D matrix showed decreased TEER.<sup>24,25,38</sup> This could be partially explained by the increase in the surface area of the 3D villi model, but also by the reduction in the expression of occludin, which is a transmembrane protein located at tight junctions and has a role in maintaining barrier function.<sup>46,47</sup> We also examined the expression of occludin in the 3D villi model and verified that occludin showed differential expression depending on the location. In particular, the expression of occludin was reduced in the villi tip area, whereas the crypt area showed a level of expression similar to that of the 2D model. The change in the barrier integrity was further supported by the significantly higher value of permeability to FITC-dextran (4 kDa) in the 3D villi model than in the 2D model. When the 3D villi model was further challenged with siMUC17 for gene silencing, the expression of occludin was decreased, which

explains the observed increase in the permeability. However, silencing of MUC17 with siRNA resulted in only a slight change in the TEER. Studies indicate that knockdown of occludin causes an increase in the permeability of various large molecules without affecting the TEER, suggesting its selective role in the macromolecule flux.<sup>48</sup> Therefore, occludin may not be directly involved in the TEER, while it regulates the permeability of macromolecules.

## 4. Materials and methods

### 4.1. Fabrication of 3D scaffolds

3D villi scaffolds were fabricated according to the methods used in the previous study.<sup>37</sup> Collagen was extracted manually from rat tails, following the method reported by Cross *et al.*,<sup>49</sup> and was polymerized by increasing the temperature from room temperature to 37 °C. A 3D villi scaffold was fabricated with 1% collagen. The average height of the villi scaffold is approximately 400 micrometers, the diameter of the villi scaffold at the bottom is approximately 200 micrometers, and the number density of the villi is 25 holes per mm<sup>2</sup>. To attach the collagen villi to the transwell inserts (6.5 mm diameter, 0.4 µm pore size, Corning, NY, USA), approximately twenty microliters of collagen pre-gel solution was first cast onto the polyester membrane of the insert and 3D collagen villi was placed on top of the collage solution. The transwell plate containing the 3D collagen villi was placed in an incubator at 37 °C to induce polymerization of collagen and bonding of 3D collagen villi to the membrane. As a control experiment, Caco-2 cells were also cultured on a flat collagen substrate inside a transwell plate (without villi structure). First, 60 µl of collagen pre-gel solution was cast on the polyester membrane of the transwell inserts to completely cover the membrane surface. The volume of the collagen pre-gel solution was determined to match the total volume of collagen under all conditions. Cells were seeded on the collagen surfaces and experiments were performed as described below.

### 4.2. Cell culture and siRNA treatment

The human colon carcinoma cell line Caco-2 (KCLB 30037, passage 30–35) was grown in the low-glucose Dulbecco's modified Eagle's medium (DMEM; Invitrogen) containing 10% fetal bovine serum (FBS; Sigma-Aldrich), and 1% penicillin/streptomycin (Sigma-Aldrich). Cells were maintained in a humidified incubator with 5% CO<sub>2</sub> at 37 °C. Trypsinized cells were seeded at a density of 5 × 10<sup>5</sup> cells per cm<sup>2</sup> onto a 3D villi scaffold (400 villus on a 4 mm × 4 mm unit square base). The 3D scaffold was then placed in a 24-well plate in the incubator with 5% CO<sub>2</sub> at 37 °C and the medium was refreshed every two days for 20 days.

To deplete the *muc17* gene, siRNA reagents containing three pooled siRNA duplexes (mRNA accession no.: NM\_001040105.1, (1) GAAGCUAGUUCAUCUUCUA, (2) CCAC-UCCGUUAGCAAGUAU, (3) CAACUCGUUGACACUAA; Bioneer, Korea) were purchased.<sup>44</sup> For siMUC17 treatment at Caco-2 cells grown on the 3D scaffold, 100 pmol of the siRNA reagents were transfected into

cell suspensions. The siRNA treatment was performed in an incubator for 5 h and repeated every two days.

### 4.3. Whole-transcriptome analysis

Trypsin was used to detach Caco-2 cells grown either in a Petri dish for three days or on the 3D villi scaffold for 20 days. Cells on the dish were directly used to extract total RNA, while cells on the 3D villi scaffold were treated with collagenase (10 µg ml<sup>-1</sup>) (Sigma Aldrich) to remove the remaining collagen components before RNA extraction. Then, total RNA was extracted from lysed cells using an RNeasy Micro Kit (Qiagen). The extracted RNA was reverse transcribed using the AccuPower CycleScript RT PreMix (Bioneer). Whole-transcriptome, high-throughput RNA sequence analysis was conducted using the synthesized cDNA fragments (Bioneer).

### 4.4. Immunostaining of MUC17 and occludin

Rabbit anti-MUC17 antibody (Sigma-Aldrich) was used to monitor MUC17 expression and localization in Caco-2 cells grown either in a Petri dish for three days or on the 3D villi scaffold for 20 days with/without siMUC17 treatment. In detail, cells in a Petri dish or a 3D villi scaffold were gently rinsed three times with PBS (phosphate buffered saline) and fixed with 10% neutralized formalin at room temperature for 20 min. After three washes with PBS, the cells were blocked with 1% bovine serum albumin (BSA; Invitrogen) in PBS for 30 min. They were then permeabilized with 0.1% Triton X-100 for 5 min and incubated with anti-MUC17 antibody at dilution ratio (1:200 in PBS) for 2 h. After being washed with PBS to remove unbound anti-MUC17 antibody, they were incubated with anti-rabbit FITC (fluorescein isothiocyanate)-conjugated antibody (Sigma-Aldrich) for 1 h at dilution ratio (1:500 in PBS). After removing unbound anti-rabbit FITC-conjugated antibody from the cells by three washes with PBD, the cells were first stained with rhodamine phalloidin (Invitrogen) at dilution ratio (1:200 in PBS) and later 4',6-diamidino-2-phenylindole (DAPI) (Sigma-Aldrich) at dilution ratio (1:10 000 in PBS) for 10 min and 5 min, respectively. Images of the stained cells were obtained using confocal laser scanning microscopy (CLSM) (Zeiss LSM 510, Carl Zeiss).

Mouse anti-occludin antibody (Invitrogen) was used to monitor occludin expression and localization in Caco-2 cells on the 3D villi scaffold for 20 days with/without siMUC17 treatment. In brief, cells were first incubated with mouse anti-occludin antibody at a dilution ratio (1:200 in PBS) for 1 h and PBS was used to wash away unbound antibody. Then, the cells were incubated with anti-mouse FITC-conjugated antibody (Sigma-Aldrich) at dilution ratio (1:500 in PBS) for 1 h and unbound antibody was washed away with PBS. Finally, the cells were stained with DAPI in a similar way, as described above before CLSM imaging.

### 4.5. Bacterial invasion and infection assays

Invasion assay was performed with wild-type *S. enterica* serovar Typhimurium ( $\chi$ 3339) labeled with green fluorescent protein (GFP). *S. typhimurium* was grown in Luria-Bertani broth (LB) containing ampicillin (final conc. 100 mg ml<sup>-1</sup>) by shaking at

37 °C overnight and the culture was re-inoculated at a dilution of 1:100 in fresh LB. The bacteria were grown until they reached an O.D. of 1.0, while Caco-2 cells were grown either in a Petri dish for three days or on the 3D villi scaffold with/without siMUC17 for 20 days. The bacteria were suspended in antibiotic-free DMEM and Caco-2 cells were infected with *S. typhimurium* at a multiplicity of infection (MOI) of approximately 100 bacterial cells per host cell for 2 h. These cells were first incubated with rhodamine phalloidin (1:200 in PBS) for 10 min and later incubated with DAPI (1:10 000 in PBS) for 5 min. The cells were analyzed using CLSM. Infection assay was performed with enterohemorrhagic *E. coli* O157:H7 (ATCC 43894) transformed with GFP. The microorganism was grown in a similar way with *S. typhimurium*. Caco-2 cells were infected with *E. coli* O157:H7 at MOI of 100. Before CLSM imaging, these cells were stained with rhodamine phalloidin and DAPI as mentioned above.

#### 4.6. Scanning electron microscopy (SEM) imaging

For SEM imaging, Caco-2 cells were fixed with 3.7% paraformaldehyde for 10 min, 2.5% glutaraldehyde for 2 h, and subsequently with 1% osmium tetroxide for 1 h in a sequential manner. After rinsing the samples with distilled water several times, the samples were freeze-dried and coated with 4 nm thick platinum using a sputter coater. Finally, images were taken by SEM (JSM-6700F; JEOL).

#### 4.7. Permeability assay

For TEER measurements, Caco-2 cells were grown on the polyester membrane and the 3D villi scaffold with/without siMUC17 treatment in transwell inserts at a seeding density of  $5 \times 10^5$  cells per cm<sup>2</sup>. The tight junctional integrity of cells was monitored by TEER measurement with an epithelial voltohmeter (Millipore ERS-2, Millipore, Bedford, MA) coupled with a chopstick-like electrode.

For permeability measurements, Caco-2 cells grown on the polyester membrane and the 3D villi scaffold (with/without siMUC17) were washed in HBSS (Hank's balanced salt solution). 5 mg ml<sup>-1</sup> FITC-Dextran (4 kDa; Sigma-Aldrich) was added (200 µl) to the apical surface of cells in the upper chamber, and HBSS was added (1 ml) to the lower chamber. At each time point, 100 µl of fluid from the lower chamber was taken and the amount of fluorescence was measured using a fluorescence spectrophotometer (Cary Eclipse Fluorescence Spectrophotometer, Agilent Technologies) at an excitation wavelength of 492 nm and an emission wavelength of 518 nm. The intensity values were converted to the FITC-Dextran concentration from a calibration data generated using known concentrations.

## 5. Conclusion

In this study, we fabricated a three-dimensional hydrogel scaffold mimicking the *in vivo* architecture of human intestinal villi, cultured Caco-2 cells on the 3D villi scaffold, and used the 3D villi model to study the gene expression, bacterial infection

process, and epithelial barrier properties of Caco-2 cells. Gene expression analysis indicated that culturing cells on the collagen villi scaffold induced enhancement of various mucin proteins, MUC17 in particular. Challenging the 3D villi model with *S. typhimurium* showed that the enhancement of MUC17 expression provided protection from bacterial infection, which was verified by the observation that knockdown of MUC17 resulted in the restoration of the bacterial infectivity. Inspection of cell tight junctions in the 2D monolayer and 3D villi model showed that the occludin expression decreased, thereby explaining the decrease in the TEER and increase in the permeability. Treatment with siMUC17 resulted in a further increase in the permeability but negligible change in the TEER, which supports the hypothesis that MUC17 is related to the epithelial barrier function. Our results suggest that the 3D intestinal villi model can serve as a more authentic, *in vivo*-like platform for studying the mechanism of bacterial infection and drug absorption. Furthermore, it can potentially serve as a platform for studying gut-related diseases such as inflammatory bowel disease.

## Acknowledgements

Collagen extract for this study was kindly provided by Dr Nakwon Choi at the Center for Biomicrosystems, Korea Institute of Science and Technology (KIST). This work was in part supported by the KFRI (Korea Food Research Institute, grant no.: E0121705), Cooperative Research Program (#PJ009419) for Agricultural Science & Technology Development through Rural Development Administration of Korea and 2013 Hongik University Research Fund.

## References

- P. Artursson, K. Palm and K. Luthman, Caco-2 monolayers in experimental and theoretical predictions of drug transport, *Adv. Drug Delivery Rev.*, 2001, **46**, 27–43.
- S. Mouly, C. Meune and J. F. Bergmann, Mini-series: I. Basic science. Uncertainty and inaccuracy of predicting CYP-mediated *in vivo* drug interactions in the ICU from *in vitro* models: focus on CYP3A4, *Intensive Care Med.*, 2009, **35**, 417–429, DOI: 10.1007/s00134-008-1384-1.
- T. M. Straub, J. R. Hutchison, R. A. Bartholomew, C. O. Valdez, N. B. Valentine, A. Dohnalkova, R. M. Ozanich and C. J. Bruckner-Lea, Defining cell culture conditions to improve human norovirus infectivity assays, *Water Sci. Technol.*, 2013, **67**, 863–868, DOI: 10.2166/wst.2012.636.
- M. L. Shuler, Modeling life, *Ann. Biomed. Eng.*, 2012, **40**, 1399–1407, DOI: 10.1007/s10439-012-0567-7.
- R. B. van Breemen and Y. Li, Caco-2 cell permeability assays to measure drug absorption, *Expert Opin. Drug Metab. Toxicol.*, 2005, **1**, 175–185, DOI: 10.1517/17425255.1.2.175.
- D. Y. Ren, C. Li, Y. Q. Qin, R. L. Yin, S. W. Du, F. Ye, H. F. Liu, M. P. Wang, Y. Sun, X. Li, M. Y. Tian and N. Y. Jin, Lactobacilli reduce chemokine IL-8 production in response to TNF-alpha and Salmonella challenge of Caco-2 cells,

- BioMed Res. Int.*, 2013, **2013**, 925219, DOI: 10.1155/2013/925219.
- 7 G. Nolleaux, C. Deville, B. El Moualij, W. Zorzi, P. Deloyer, Y. J. Schneider, O. Peulen and G. Dandrifosse, Development of a serum-free co-culture of human intestinal epithelium cell-lines (Caco-2/HT29-5M21), *BMC Cell Biol.*, 2006, **7**, 20, DOI: 10.1186/1471-2121-7-20.
  - 8 A. G. Mikos, S. W. Herring, P. Ochareon, J. Elisseeff, H. H. Lu, R. Kandel, F. J. Schoen, M. Toner, D. Mooney, A. Atala, M. E. Van Dyke, D. Kaplan and G. Vunjak-Novakovic, Engineering complex tissues, *Tissue Eng.*, 2006, **12**, 3307–3339, DOI: 10.1089/ten.2006.12.3307.
  - 9 L. G. Griffith and M. A. Swartz, Capturing complex 3D tissue physiology *in vitro*, *Nat. Rev. Mol. Cell Biol.*, 2006, **7**, 211–224, DOI: 10.1038/nrm1858.
  - 10 K. M. Yamada and E. Cukierman, Modeling tissue morphogenesis and cancer in 3D, *Cell*, 2007, **130**, 601–610, DOI: 10.1016/j.cell.2007.08.006.
  - 11 A. Abbott, Cell culture: biology's new dimension, *Nature*, 2003, **424**, 870–872, DOI: 10.1038/424870a.
  - 12 M. C. Cushing and K. S. Anseth, Materials science, Hydrogel cell cultures, *Science*, 2007, **316**, 1133–1134, DOI: 10.1126/science.1140171.
  - 13 D. Choudhury, X. Mo, C. Iliescu, L. L. Tan, W. H. Tong and H. Yu, Exploitation of physical and chemical constraints for three-dimensional microtissue construction in microfluidics, *Biomicrofluidics*, 2011, **5**, 22203, DOI: 10.1063/1.3593407.
  - 14 J. H. Sung, M. B. Esch, J. M. Prot, C. J. Long, A. Smith, J. J. Hickman and M. L. Shuler, Microfabricated mammalian organ systems and their integration into models of whole animals and humans, *Lab Chip*, 2013, **13**, 1201–1212, DOI: 10.1039/c3lc41017j.
  - 15 J. Lee, G. D. Lilly, R. C. Doty, P. Podsiadlo and N. A. Kotov, *In vitro* toxicity testing of nanoparticles in 3D cell culture, *Small*, 2009, **5**, 1213–1221, DOI: 10.1002/smll.200801788.
  - 16 A. S. Kienhuis, H. M. Wortelboer, J. C. Hoflack, E. J. Moonen, J. C. Kleinjans, B. van Ommen, J. H. van Delft and R. H. Stierum, Comparison of coumarin-induced toxicity between sandwich-cultured primary rat hepatocytes and rats *in vivo*: a toxicogenomics approach, *Drug Metab. Dispos.*, 2006, **34**, 2083–2090, DOI: 10.1124/dmd.106.011262.
  - 17 P. A. Kenny and M. J. Bissell, Tumor reversion: correction of malignant behavior by microenvironmental cues, *Int. J. Cancer*, 2003, **107**, 688–695, DOI: 10.1002/ijc.11491.
  - 18 K. L. Schmeichel and M. J. Bissell, Modeling tissue-specific signaling and organ function in three dimensions, *J. Cell Sci.*, 2003, **116**, 2377–2388, DOI: 10.1242/jcs.00503.
  - 19 M. Papadaki, N. Bursac, R. Langer, J. Merok, G. Vunjak-Novakovic and L. E. Freed, Tissue engineering of functional cardiac muscle: molecular, structural, and electrophysiological studies, *Am. J. Physiol.: Heart Circ. Physiol.*, 2001, **280**, H168–H178.
  - 20 C. E. Holy, M. S. Shoichet and J. E. Davies, Engineering three-dimensional bone tissue *in vitro* using biodegradable scaffolds: investigating initial cell-seeding density and culture period, *J. Biomed. Mater. Res.*, 2000, **51**, 376–382.
  - 21 J. K. Nicholson, E. Holmes and I. D. Wilson, Gut microorganisms, mammalian metabolism and personalized health care, *Nat. Rev. Microbiol.*, 2005, **3**, 431–438, DOI: 10.1038/nrmicro1152.
  - 22 J. P. Medema and L. Vermeulen, Microenvironmental regulation of stem cells in intestinal homeostasis and cancer, *Nature*, 2011, **474**, 318–326, DOI: 10.1038/nature10212.
  - 23 C. P. Gayer and M. D. Basson, The effects of mechanical forces on intestinal physiology and pathology, *Cell. Signalling*, 2009, **21**, 1237–1244, DOI: 10.1016/j.cellsig.2009.02.011.
  - 24 N. Li, D. Wang, Z. Sui, X. Qi, L. Ji, X. Wang and L. Yang, Development of an improved three-dimensional *in vitro* intestinal mucosa model for drug absorption evaluation, *Tissue Eng., Part C*, 2013, **19**, 708–719, DOI: 10.1089/ten.TEC.2012.0463.
  - 25 F. Leonard, E. M. Collnot and C. M. Lehr, A three-dimensional coculture of enterocytes, monocytes and dendritic cells to model inflamed intestinal mucosa *in vitro*, *Mol. Pharmaceutics*, 2010, **7**, 2103–2119, DOI: 10.1021/mp1000795.
  - 26 T. M. Straub, R. A. Bartholomew, C. O. Valdez, N. B. Valentine, A. Dohnalkova, R. M. Ozanich, C. J. Bruckner-Lea and D. R. Call, Human norovirus infection of Caco-2 cells grown as a three-dimensional tissue structure, *J. Water Health*, 2011, **9**, 225–240.
  - 27 A. L. Radtke, J. W. Wilson, S. Sarker and C. A. Nickerson, Analysis of interactions of Salmonella type three secretion mutants with 3-D intestinal epithelial cells, *PLoS One*, 2010, **5**, e15750, DOI: 10.1371/journal.pone.0015750.
  - 28 J. Pusch, M. Votteler, S. Gohler, J. Engl, M. Hampel, H. Walles and K. Schenke-Layland, The physiological performance of a three-dimensional model that mimics the microenvironment of the small intestine, *Biomaterials*, 2011, **32**, 7469–7478, DOI: 10.1016/j.biomaterials.2011.06.035.
  - 29 H. J. Kim and D. E. Ingber, Gut-on-a-Chip microenvironment induces human intestinal cells to undergo villus differentiation, *Integr. Biol.*, 2013, **5**, 1130–1140, DOI: 10.1039/c3ib40126j.
  - 30 H. J. Kim, D. Huh, G. Hamilton and D. E. Ingber, Human gut-on-a-chip inhabited by microbial flora that experiences intestinal peristalsis-like motions and flow, *Lab Chip*, 2012, **12**, 2165–2174, DOI: 10.1039/c2lc40074j.
  - 31 Y. Y. Fu, C. W. Lin, G. Enikolopov, E. Sibley, A. S. Chiang and S. C. Tang, Microtome-free 3-dimensional confocal imaging method for visualization of mouse intestine with subcellular-level resolution, *Gastroenterology*, 2009, **137**, 453–465, DOI: 10.1053/j.gastro.2009.05.008.
  - 32 L. Wang, S. K. Murthy, W. H. Fowle, G. A. Barabino and R. L. Carrier, Influence of micro-well biomimetic topography on intestinal epithelial Caco-2 cell phenotype, *Biomaterials*, 2009, **30**, 6825–6834, DOI: 10.1016/j.biomaterials.2009.08.046.
  - 33 L. Wang, S. K. Murthy, G. A. Barabino and R. L. Carrier, Synergic effects of crypt-like topography and ECM proteins on intestinal cell behavior in collagen based membranes, *Biomaterials*, 2010, **31**, 7586–7598, DOI: 10.1016/j.biomaterials.2010.06.036.
  - 34 M. B. Esch, J. H. Sung, J. Yang, C. Yu, J. Yu, J. C. March and M. L. Shuler, On chip porous polymer membranes for

- integration of gastrointestinal tract epithelium with microfluidic 'body-on-a-chip' devices, *Biomed. Microdevices*, 2012, **14**, 895–906, DOI: 10.1007/s10544-012-9669-0.
- 35 C. M. Costello, J. Hongpeng, S. Shaffiey, J. Yu, N. K. Jain, D. Hackam and J. C. March, Synthetic small intestinal scaffolds for improved studies of intestinal differentiation, *Biotechnol. Bioeng.*, 2014, **111**, 1222–1232, DOI: 10.1002/bit.25180.
- 36 C. M. Costello, R. M. Sorna, Y. L. Goh, I. Cengic, N. K. Jain and J. C. March, 3-d intestinal scaffolds for evaluating the therapeutic potential of probiotics, *Mol. Pharmaceutics*, 2014, **11**, 2030–2039, DOI: 10.1021/mp5001422.
- 37 J. H. Sung, J. Yu, D. Luo, M. L. Shuler and J. C. March, Microscale 3-D hydrogel scaffold for biomimetic gastrointestinal (GI) tract model, *Lab Chip*, 2011, **11**, 389–392, DOI: 10.1039/c0lc00273a.
- 38 J. Yu, S. Peng, D. Luo and J. C. March, *In vitro* 3D human small intestinal villous model for drug permeability determination, *Biotechnol. Bioeng.*, 2012, **109**, 2173–2178, DOI: 10.1002/bit.24518.
- 39 N. Moniaux, W. M. Junker, A. P. Singh, A. M. Jones and S. K. Batra, Characterization of human mucin MUC17. Complete coding sequence and organization, *J. Biol. Chem.*, 2006, **281**, 23676–23685, DOI: 10.1074/jbc.M600302200.
- 40 K. L. Carraway, V. P. Ramsauer, B. Haq and C. A. Carothers Carraway, Cell signaling through membrane mucins, *BioEssays*, 2003, **25**, 66–71, DOI: 10.1002/bies.10201.
- 41 M. A. Hollingsworth and B. J. Swanson, Mucins in cancer: protection and control of the cell surface, *Nat. Rev. Cancer*, 2004, **4**, 45–60, DOI: 10.1038/nrc1251.
- 42 M. Andrianifahanana, N. Moniaux and S. K. Batra, Regulation of mucin expression: mechanistic aspects and implications for cancer and inflammatory diseases, *Biochim. Biophys. Acta*, 2006, **1765**, 189–222, DOI: 10.1016/j.bbcan.2006.01.002.
- 43 Y. Luu, W. Junker, S. Rachagani, S. Das, S. K. Batra, R. L. Heinrikson, L. L. Shekels and S. B. Ho, Human intestinal MUC17 mucin augments intestinal cell restitution and enhances healing of experimental colitis, *Int. J. Biochem. Cell Biol.*, 2010, **42**, 996–1006, DOI: 10.1016/j.biocel.2010.03.001.
- 44 S. Resta-Lenert, S. Das, S. K. Batra and S. B. Ho, Muc17 protects intestinal epithelial cells from enteroinvasive E. coli infection by promoting epithelial barrier integrity, *Am. J. Physiol.: Gastrointest. Liver Physiol.*, 2011, **300**, G1144–G1155, DOI: 10.1152/ajpgi.00138.2010.
- 45 P. L. Devine and I. F. McKenzie, Mucins: structure, function, and associations with malignancy, *BioEssays*, 1992, **14**, 619–625, DOI: 10.1002/bies.950140909.
- 46 B. E. Phillips, L. Cancel, J. M. Tarbell and D. A. Antonetti, Occludin independently regulates permeability under hydrostatic pressure and cell division in retinal pigment epithelial cells, *Invest. Ophthalmol. Visual Sci.*, 2008, **49**, 2568–2576, DOI: 10.1167/iovs.07-1204.
- 47 T. Hirase, S. Kawashima, E. Y. Wong, T. Ueyama, Y. Rikitake, S. Tsukita, M. Yokoyama and J. M. Staddon, Regulation of tight junction permeability and occludin phosphorylation by Rhoa-p160ROCK-dependent and -independent mechanisms, *J. Biol. Chem.*, 2001, **276**, 10423–10431, DOI: 10.1074/jbc.M007136200.
- 48 R. Al-Sadi, K. Khatib, S. Guo, D. Ye, M. Youssef and T. Ma, Occludin regulates macromolecule flux across the intestinal epithelial tight junction barrier, *Am. J. Physiol.: Gastrointest. Liver Physiol.*, 2011, **300**, G1054–G1064, DOI: 10.1152/ajpgi.00055.2011.
- 49 V. L. Cross, Y. Zheng, N. Won Choi, S. S. Verbridge, B. A. Sutermaster, L. J. Bonassar, C. Fischbach and A. D. Stroock, Dense type I collagen matrices that support cellular remodeling and microfabrication for studies of tumor angiogenesis and vasculogenesis *in vitro*, *Biomaterials*, 2010, **31**, 8596–8607, DOI: 10.1016/j.biomaterials.2010.07.072.